Potential Impact of Carbon Nanotube Reinforced Polymer Composite on Commercial Aircraft Performance and Economics

Sarah E. O'Donnell,* Kevin R. Sprong† and Brennan M. Haltli†
The MITRE Corporation, McLean, Virginia, 22102

This study investigates the potential performance impact of incorporating carbon nanotube reinforced polymer (CNRP) composites in four present-day airframes. Flight profiles of current and notional 70% single-walled carbon nanotube (SWNT) by volume carbon nanotube reinforced polymer (CNRP) structured airframes are modeled through the utilization of Euro Control's Base of Aircraft Data (BADA) and from traditional flight dynamics theory. Using this data, flights are constructed from takeoff to landing and fuel consumption is evaluated. Due to the decrease in structural mass from aluminum airframes to notional CNRP-structured airframes of 14.05% on average, observed results include consequential decrease in fuel consumption by an average of 09.8% and an increase in flight range by an average of 13.2%. Flight path data from the Enhanced Traffic Management System (ETMS) enables a correlation of fuel consumption savings to actual fuel savings for common flight paths for the aircraft types investigated in this study.

Nomenclature

α	=	composite stress index
$\boldsymbol{a_1}$	=	unit vector
$\boldsymbol{a_2}$	=	unit vector
$\boldsymbol{C_h}$	=	chiral vector
M_{AT}	=	aircraft mass at takeoff
M_F	=	maximum fuel load
M_L	=	maximum aircraft payload
M_{OE}	=	aircraft operating empty weight
m	=	integer number of carbon atoms in $\mathbf{a}_2$ direction
n	=	integer number of carbon atoms in $\mathbf{a}_1$ direction
V_{fiber}	=	volume fraction of high-modulus composite reinforcement phase
$X_{composite}$	=	mechanical property placeholder for the composite
X_{fiber}	=	mechanical property placeholder for the high-modulus composite reinforcement phase
X_{matrix}	=	mechanical property placeholder for the low-modulus composite binding phase

I. Introduction

AIRCRAFT design favors materials with high specific strengths (strength/density),[1] which reduce aircraft mass while maintaining airframe structural integrity. Many present-day aircraft structures take advantage of the specific strength benefits of aluminum alloys, such as 2024-T3, for the fuselage and graphite-epoxy composites for the empennage and control surfaces,[5] such as in the Boeing 747-400. Although commercial aircraft from the Federal Aviation Administration's (FAAs) "heavy" category, such as the 747-400, are primarily structured with aluminum alloys, future designs for the Boeing 7E7 include graphite-epoxy composites as the primary structural material.[6, 7] A new composite, reinforced by nanoscopic fibers, may provide aircraft designers with another structural material option for airframes.

* Simulation Modeling Engineer, Senior, Center for Advanced Aviation Systems Development, 7515 Colshire Drive/N390, AIAA Member.
† Simulation Modeling Engineer, Center for Advanced Aviation Systems Development, 7515 Colshire Drive/N390.

The nanoscopic fibers, known as carbon nanotube molecules are a new form of elemental carbon with intriguing properties. For example, the strongest tubes exhibit roughly eighty times the strength, six times the toughness, or Young's Modulus, and one-sixth the density of high carbon steel. Utilizing the carbon nanotube as a molecular "fiber" in a carbon nanotube reinforced polymer (CNRP) provides a potentially favorable material for aerospace applications.

Carbon fiber composites tend to be less dense than metals, and often provide improved strength and corrosion protection. Carbon nanotube composites will likely provide a low density, corrosion resistant composite that can be used in lower volumes due to the curious mechanical properties of the carbon nanotube, especially its strength, modulus, and conductivity. Incorporating CNRP composites in an airframe potentially offers each of these advantages to the aircraft. Benefits can be seen immediately, without airframe redesign which considers the material strength and modulus properties, by observing the performance and efficiency benefits of weight reduction due to the low density of CNRP.

The analysis presented here considers a notional Boeing 747-400 and 757-200, Airbus A320, and Embraer E145 with CNRP as the primary structural material, replacing the entire volume of structural aluminum with CNRP, without including any modifications to the geometry or design of the airframe. Though the probability of a CNRP-structured contemporary airframes is unlikely, this type of analysis provides insight into a small group of benefits seen by a nano-structured material applied on the macro scale.

This paper discusses the carbon nanotube molecule, its use in a composite material (CNRP), and the potential impacts of CNRP on current commercial airframes. First, a brief background on carbon nanotubes is provided. It is followed by a discussion of the theoretical calculations and analysis used to find the mechanical properties of CNRP including Young's modulus, tensile strength, and density as compared to those found in literature. Using the calculated CNRP mechanical properties, a mass reduction for the 747-400, 757-200, A320, and E145 due to CNRPs specific strength is estimated. Finally, an analysis is performed of the impact of this mass reduction on the aircraft's performance, fuel consumption, and economic flight profile.

II. Carbon Nanotube Reinforced Polymer

A. The Carbon Nanotube

Some scientists claim the carbon nanotube to be "the strongest material that will ever be made."[8] Pure single-walled nanotubes (SWNT) characteristically exhibit the highest toughness, or Young's modulus, peaking around 1.25 Tera Pascal, (TPa). [4,9-10] This molecule is tougher than spider silk, whose Young's modulus nears 300 Mega Pascal, MPa.[11] Although both single and multi-walled nanotubes (MWNT) exhibit outstanding strength and modulus, pure SWNT prove exceptional as reinforcing "fibers" for a carbon nanotube reinforced polymer composite. [12-14]

Figure 1. Wire Frame Model of a Single-Walled Carbon Nanotube (SWNT) Molecular Structure. *Notice the chicken-wire like lattice structure of what appears to be a graphene sheet rolled into a tubule.*

Carbon nanotubes have various chiralities, or "twists," in the graphene lattice which define the tube structure.[15] The angle of twist is directly related to the chiral vector, C_h, which is defined by the vector addition of two normalized (unit) vectors, a_1 and a_2, and their respective indices (m,n) as shown in the following equation:

$$\mathbf{C_h} = n\mathbf{a_1} + m\mathbf{a_2} \tag{1}$$

Because mechanical properties of the (10,10) armchair carbon nanotube have been theoretically[19] and experimentally[3,4] observed, it is the molecular nanotube of choice for this analysis. Fig. 2 illustrates the chiral vector for an armchair nanotube, where $m = n = 10$. The name "armchair" originates from the geometry of the nanotube bonds around the tube circumference.

Armchair SWNTs behave as metals.[16,17] Conductivity in metallic nanotubes occurs via ballistic electron transport, resulting in high current carrying capacity with little energy sacrifice to heat.[18]

The Young's modulus for a (10,10) armchair SWNT averages approximately 640 GigaPascal (GPa) according to calculations[19] and measurements.[3] SWNT bundles exhibit tensile strengths that range from approximately 15 to 52 GPa and a corresponding tensile strain minimum of 5.3%, where the load is applied to the nanotubes at the perimeter of each bundle.[3,20] Multi-walled nanotubes range in tensile strength from 11 to 63 GPa, with a tensile strain at fracture[21-22] of close to 12%.

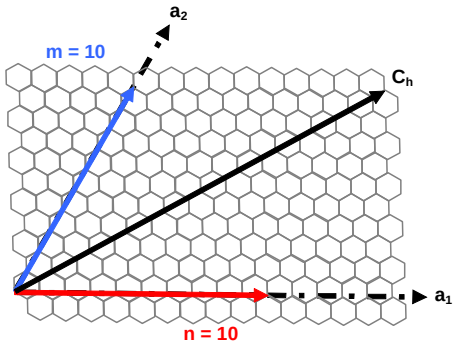

Figure 2. (10,10) Armchair Nanotube Chiral Vector Diagram. *A formed (10,10) armchair carbon nanotube appears as a tube rolled seamlessly along the chiral vector C_h. The chiral vector shows the direction of "twist" and circumference of the tubular*

Table 1. Mechanical Properties of High- and Low-Modulus Phases of CNRP. *High Density Polyethylene serves as the low modulus phase, and Single-Walled Carbon Nanotube as the high-modulus phase. For more conservative calculations, the mean values of mechanical properties of SWNT are used in the analysis; denoted by <SWNT>. Optimal values for SWNT are also presented.*

Material Type	Density (kg/m³)	Youngs Modulus (Gpa)	Tensile Strength (Gpa)
HDPE[23]	955	2.40	0.021
<SWNT>[9,19,3]	1300	640	37.0
SWNT[9,4,3]	1300	1200	50.0

B. Carbon Nanotube Reinforced Polymer Composite

Classically, composites consist of a high-modulus fiber in a low-modulus matrix, where the fiber toughens and strengthens the binding material, or matrix. Due to their exceptional mechanical properties, (10,10) SWNT are commonly used as the reinforcing fiber in carbon nanotube composite,[12-14] and will be used for the CNRP property estimates to follow.

In this analysis, the density, tensile strength, and Young's modulus are known for the polymer matrix and the nanotube molecule. The following analysis includes high density polyethylene (HDPE) as the polymer matrix material, or low modulus phase, and (10,10) SWNT as the high modulus phase. The material properties of HDPE and SWNT are listed in Table 1.

Several methods exist for calculating mechanical properties of composites, including the method of mixtures (MOM).[1,25] MOM is used as a first order approximation in this research[26] to estimate the density, tensile strength, and Young's modulus of bi-directional CNRP. The evenly aligned, dispersed fibers of a bi-directional composite, illustrated in Fig. 3, fall under the category of a uniformly dispersed, aggregate composite commonly analyzed by MOM.[1,25,27] MOM enables the analysis of materials on the macro-scale when given the bulk mechanical properties, including tensile strength, modulus, diffusivity, thermal conductivity, or electrical conductivity[1] of the composite's constituents.

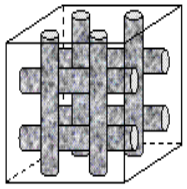

Figure 3. Bi-Directional Composite Structure. *The reinforcing fibers are oriented at 0˚ and 90˚ in the polymer matrix.*

The general equation for the method of mixtures is:

$$X_{composite} = \left[V_{fiber} X_{fiber}^{\alpha} + \left(1 - V_{fiber}\right) X_{matrix}^{\alpha}\right]^{1/\alpha} \quad (2)$$

where V is volume fraction, X is the mechanical property, and α is the stress index.[1] The CNRP mechanical property analysis includes a range of three SWNT volume fractions: 50, 60, and 70% in HDPE. It is interesting to note that present-day, commercially available common graphite-epoxy composite consists of 66-70% volume fraction graphite fibers in epoxy.[27]

Evaluating at α = 1, indicates a unidirectional composite where the force is applied parallel to the axis of the fibers, placing the material in isostrain as illustrated in Figure 4a. Evaluating at α = -1 indicates a unidirectional composite where the force is applied orthogonal to the axis of the fiber orientation, placing the material in isostress as illustrated in Fig. 4b. Evaluating equation (1) within boundary values, $-1 < \alpha < 1$, produces mechanical property estimates for a bidirectional composite with orthogonally oriented fibers as seen in Fig. 3, existing in the isostrain and isostress condition with the load applied on either fiber orientation axis.

Evaluating Equation (1) for Young's modulus, tensile strength, and density at α = 0.01 provides a first order approximation for a bi-directional composite of orthogonal fiber orientation with a higher-modulus fiber in a lower-modulus matrix.[1] As seen in Table 2, the following results are for the SWNT volume fractions, producing a range of results for bi-directional CNRP used in the aircraft structure analysis in Section C.

Experimental CNRP findings by other investigators show consistent values for material mechanical properties vary[32-35] due to several factors, including experimental apparatus, SWNT dimensions, SWNT density measurement, the ability to uniformly disperse nanotubes throughout the matrix, and differences in the purity of SWNT.[35] Some investigators have been focusing on spinning the nanotube molecules into fibers, much as spiders spin silk, to weave fabrics used in composite laminate layers.[36-38] Some of these same findings exhibit only a slight improvement over the mechanical properties of current carbon fiber composites.[32]

As dispersion becomes more uniform and isolating SWNT from bundles does not affect their purity, experimental CNRP properties will potentially approach those predicted theoretically, providing improved values over the results illustrated in the first order approximation in this study and more accurate continuum and constitutive models from other studies. Such a possible improvement over current structural materials might mean that CNRP will replace existing alloys and composites without compromising added weight for strength and toughness, leading to improvements in the performance of the vehicles which use CNRP in their structures.

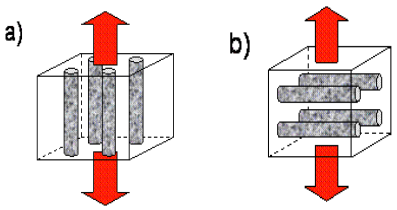

Figure 4. Composite Axial Loading. *a) Unidirectional composite in isostrain. The uniaxial load is applied parallel to the reinforcing fibers. b) Unidirectional composite in isostress. The uniaxial load is applied orthogonal to the reinforcing fibers.*

Table 2. CNRP Mechanical Properties at Selected Single Walled Carbon Nanotube (SWNT) Volume Fractions. *CNRP Constituent properties are found in Table 1. HDPE is the low-modulus matrix phase and CNRP is the high-modulus "fiber" phase.*

CNRP % SWNT	Density (kg/m³)	Young's Modulus (Gpa)	Tensile Strength (Mpa)
50	1130	57.6	1740
60	1160	97.9	3470
70	1200	162	6620

Table 3. Mechanical Properties of Common Structural Materials. *AISI 1040 Rolled Steel[28] Ti-13V-11Cr-3Al solution treated, Age 4500˚C Titanium[29] (used on SR-71 Blackbird);[30] 2024-T3 Aluminum;[31] Thornel 300 graphite fibers in Narmco 5208 epoxy for T300/5208 CFRP.[27]*

Material Type	Density (kg/m³)	Youngs Modulus (Gpa)	Tensile Strength (Mpa)
Steel	7845	200	620
Titanium	4820	110	1170
Aluminum	2780	73	480
CFRP‡	1600	181	1500

C. Mass Analysis of CNRP-Structured Aircraft

Using CNRP in aircraft structures has several predictable impacts on aircraft design. The most obvious of which is significant airframe weight reduction stemming from CNRPs low density and complemented by its high strength

‡ Carbon Fiber Reinforced Polymer

and modulus presented in Table 1 of Section B. To demonstrate this potential, a notional CNRP-structured present day Boeing 747-400, 757-200, Airbus A320, and Embraer 145 commercial airframes are analyzed.

It is understood that re-constructing present-day aircraft with CNRP airframes is a highly unlikely future scenario. However, because future aircraft designs remain uncertain, examining the impact CNRP may have on today's aircraft provides insight into potential future aircraft performance and designs.

To illustrate the likely impact of reduced 747-400 airframe weight from utilizing CNRP, the volume of structural aluminum in each airframe is replaced with an equivalent volume of CNRP. Multiplying the mass of 2024-T3 aluminum in the structure[39] by its density provides the volume of structural material considered in the analysis. Type 2024-T3 Aluminum is a common material used in commercial jet aircraft.[30] Then, the mass of CNRP is determined by multiplying the volume of structural material by the density of CNRP. This calculation is performed for three SWNT volume fraction-dependent densities to obtain three structural CNRP masses. Although a lower volume of CNRP would likely exist because of its strength and resilience, this analysis does not account for the re-design of specific structural elements involved. Other structural characteristics, especially airfoil and fuselage geometry, remain as found in the original aircraft structures.

The evaluation to follow applies the assumptions and structural mass projections for the notional CNRP-structured airframes included above to an aircraft mass analysis. In Section D, performance characteristics, such as fuel efficiency, aircraft range, flight duration, cruise altitude, and economic flight profiles resulting from the change in aircraft mass are evaluated and discussed.

The mass reduction analysis compares Mass At Takeoff (M_{AT}) values from the original aircraft to calculated CNRP M_{AT} values. Data from Euro Control's Base of Aircraft Data,[49] or BADA, provides three M_{AT} for each airframe and associated fuel consumption rates, cruise altitudes and speeds. Each data set includes M_{AT}, with operating empty weight (OEW or M_{OE}), maximum payload (M_L), and maximum fuel load (M_F) found from manufacturer's data. OEW is the only value that remains constant for the low, moderate, and high present-day aircraft masses. The fuel and payload are the primary contributors to the mass differentiation in the data sets, and the differentiation is primarily between air carriers using the same airframe.

The CNRP aircraft mass analysis is based on the low, moderate, and high mass data as well as the CNRP material property results from the previous section. To calculate the range of CNRP M_{AT}, the CNRP operating empty weights[40] (OEW) are found for each of the SWNT volume fractions. This calculation subtracts the mass of structural aluminum, and adds in each of the three new CNRP masses to obtain a range of CNRP OEWs shown in Table 4.

Table 4. Range of CNRP 747-400 Operating Empty Weights (OEWs). *The study focuses on 70% SWNT CNRP notional airframes where the weight reduction occurs in the fraction of M_{OE} (kg) containing structural aluminum.*

Material		OEW (kg)
Aluminum		179015
CNRP %SWNT	50	139800
	60	140600
	70	**141400**

Then, for each of the OEWs calculated, the low, moderate, and high BADA data are applied using the following equation:[41]

$$M_{AT} = M_{OE} + M_F + M_L \tag{3}$$

to obtain a matrix of possible CNRP M_{TO} shown in Table 5. This matrix of CNRP structured aircraft takeoff masses is applied to the performance and efficiency analysis.

This analysis focuses on the 70% SWNT CNRP. Table 5 shows each of the four aircraft types evaluated with CNRP structures as compared to their contemporary aluminum counterparts. Table 5 illustrates CNRP structured airframe M_{AT} ranges for low, moderate, and high masses at 70% SWNT volume fraction as compared to the original aluminum-structured airframes. Mass savings within aircraft types goes from 17.5% less mass with the Low 747-400 aircraft to 10.1% less mass in the Hi 747-400. Mass reduction due to CNRP is more substantial for the low mass airframes, as the increase in mass from low to high within aircraft type is due to an increase in either fuel load or payload. Average fuel savings for all category aircraft is 14.05%.

Table 5. Percent Reduction in Airframe Mass by Swapping Aluminum with CNRP. *Most significant mass saving for each aircraft occurs between "Low" mass categories. Additional weight from Nominal to High cases within the same material class is due to fuel and payload.*

	Percent Mass Reduction from Aluminum- to CNRP-structured Airframes		
	Low	***Nom***	***Hi***
747-400	17.54	12.63	10.19
757-200	17.37	13.08	10.75
A320	17.62	14.26	12.03
E145	16.76	14.31	12.17

BADA data for flight profiles are used in conjunction with theory of flight dynamics to calculate fuel consumption and related impacts, and new aircraft perating envelopes to analyze the impact of the weight reduction due to CNRP on the aircraft.

D. CNRP Aircraft Performance

Weight reduction directly affects aircraft performance, economics, and efficiency. This should be true, even assuming no change in aircraft geometry. To test this thesis with regards to CNRP-structured airframes, several further analyses are performed. Fuel efficiency and aircraft range are analyzed for both aluminum and CNRP airframes. Then, typical flight routes for each aircraft are modeled and fuel consumption analyzed to compare with current fuel consumption and range numbers. This information is fed into an economics analysis to provide information on potential monetary savings due to such efficiencies.

1. Aircraft Range with Constant Fuel Consumption

To model the fuel efficiency increases for CNRP structured aircraft, BADA data is used to construct a flight from takeoff to landing, using the rates of climb, cruise speed, and rates of descent, in addition to fuel burn rates for all the phases of flight. In this way, an entire flight profile for an aircraft may be modeled. As with other analyses, the 70% SWNT by volume CNRP is evaluated, as that is the most common ratio of carbon fiber to HDPE in carbon fiber reinforced polymer. Modeling includes present-day aluminum structured aircraft versus the CNRP structured aircraft in several scenarios.

In the first scenario analyzed, the aircraft would take off with maximum rated fuel loading and fly until 20% of the original fuel load remains. Cruise altitudes were chosen from actual flight statistical data. These altitudes, on average, corresponded to a flight level 4000 feet below the maximum listed flight level in BADA. Using this flight profile, the range increase possible for each aircraft is ascertained, holding fuel consumption constant. The summary of flight distance for each aircraft under these conditions is presented below in Table 6.

There are two cases analyzed for the CNRP structured aircraft, one in which the standard case aircraft cruise at the same altitude as the CNRP aircraft, and one in which the lighter airframe provided by the carbon nanotube structure allows for a higher cruise

Table 6. Flight Distance for Aircraft with Constant Fuel Consumption

Distance flown with constant fuel consumption (nmi)			
Airframe		**Case**	
	Low		
	Aluminum	***70% SWNT Std. Cruise***	***70% SWNT Higher Cruise***
747-400	7671	8070	9091
757-200	4072	4438	4969
A320	3032	3385	3497
E145	1008	1066	1549
	Nom		
	Aluminum	***70% SWNT Std. Cruise***	***70% SWNT Higher Cruise***
747-400	6333	6404	8584
757-200	3329	3498	3812
A320	2757	3038	3123
E145	1185	1243	1307
	Hi		
	Aluminum	***70% SWNT Std. Cruise***	***70% SWNT Higher Cruise***
747-400	6396	6415	x
757-200	2882	2994	x
A320	2492	2754	2815
E145	1257	1322	1828

profile (The 'Hi' case was not analyzed for the B747-400 nor for the B757-200 in this scenario, as BADA data for the 'Hi' case did not exist at the better cruise altitudes for these aircraft).[49] This may provide an additional benefit to our CNRP-structured aircraft, since all other things being equal, lighter aircraft perform more optimally at higher altitudes.

In addition to the extended distance benefit, there are also airspace benefits that require further study and are not addressed in detail in this analysis. In essence, the potential for four more available flight levels for en route aircraft may be opened with further evaluation of CNRP aircraft performance in airspace.

However, the fuel efficiency results, in terms of nautical mile per volumetric consumption of fuel, are straightforward and one example result is illustrated in Fig. 5, where the CNRP structured Embraer-145 achieves (on average) a range increase of 5 % versus the aluminum airframe. By using the higher cruise altitude, denoted "better cruise," allowed by the lighter airframe, the range increase jumps to 36 %. The average flight range increase for all category aircraft is 13.2%.

Figure 5. Increase in CNRP Structured Embraer 145 Range over the Aluminum-Structured Airframe. *As modeled, the notional CNRP-Structured Embraer 145 travels close to 36% further than its contemporary counterpart, and cruises higher.*

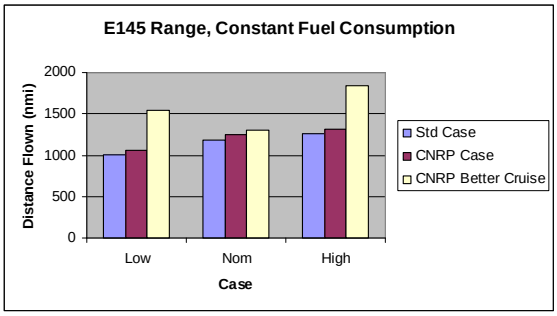

2. Fuel Efficiency with Constant Aircraft Range

The second scenario involved modeling each aircraft flight over a set distance; here the response variable is fuel consumed. For this initial assessment of fuel savings, the distance that the standard case aircraft flies in the first scenario is used: the distance flown with 20% of its initial fuel load remaining. Then the CNRP aircraft's flight distances are matched up to these, again using both standard and better (higher) CNRP cruise altitude profiles. Results are presented in Table 7.

Table 7. Fuel Consumption of Select Aluminum and CNRP–Structured Aircraft over Constant Range.

Fuel consumed with constant range (kg)			
Airframe		**Case**	
	Low		
	Aluminum	***70% SWNT Std. Cruise***	***70% SWNT Higher Cruise***
747-400	130149	123830	110165
757-200	27418	25265	22687
A320	15326	13789	13381
E145	3347	3158	2247
	Nom		
	Aluminum	***70% SWNT Std. Cruise***	***70% SWNT Higher Cruise***
747-400	130572	129165	97140
757-200	27395	26150	24128
A320	15327	13970	13672
E145	4163	3965	2858
	Hi		
	Aluminum	***70% SWNT Std. Cruise***	***70% SWNT Higher Cruise***
747-400	154464	153882	x
757-200	27436	26442	x
A320	15326	13938	13664
E145	4770	4542	3359

The gains here strongly correlate with the range increases for each aircraft, for both the equal cruise and better CNRP cruise scenarios, which follows from the direct relation of fuel consumption and flight distance. The low mass, better (higher) cruising Embraer 145 shows the most promise, saving close to one-third the total fuel mass consumed by the contemporary counterpart. The average fuel mass savings for the A320, E145, B747-400, and B757-200 are 10.38%, 14.14%, 5.81%, and 9.01%, respectively. The average fuel savings among the group of four CNRP-structured airframes nears 9.8%.

3. Economic Gains Based on Current Routes Flown

To get a better understanding of the potential economic impact of CNRP from a fuel consumption standpoint, four aircraft flights are modeled over actual routes used by the four contemporary aircraft observed in the study. To obtain data on flight operations by airframe, the Enhanced Traffic Management System (ETMS)[50] is utilized, which contains data from flights flying into and out of over 2000 airports nationwide. This gave not only the most popular routes that each of our four airframes use, but also flight distances for those routes, which were calculated from the airplane's constant latitude/longitude position updates, available from ETMS.

Using ETMS data from 5 May 2004 to 10 May 2004 to find routes, and modeling the aircraft to fly the distances provided for those routes, an estimated dollar savings per operation of the aircraft on the route is obtained. The aircraft-dependent routes for which monetary economics are evaluated are presented in Table 8, and the dollar savings[51] are presented in Table 9.

Again, there is a substantial jump in the benefit when moving to the higher cruise profile, due to the increased fuel efficiency lent at a higher altitude. Considering the large number of operations of each of these aircraft on these four routes alone, the potential for yearly savings is staggering.

The most interesting economic result comes from the higher cruising, notional CNRP-structured 747-400 of nominal weight, with a savings of nearly $10k per flight. With two flights per day, a savings of $40k for two round-trip flights potentially translates to savings for the commercial aircraft user as well as the service provider.

Table 8. Most Popular Routes for Select Aircraft

Most popular routes and their lengths		
Airframe	***Route***	***Distance***
747-400	LAX-ICN	5676 nmi
757-200	SFO-ORD	2119 nmi
A320	JFK-FLL	984 nmi
E145	IAH-DAL	241 nmi
Source : ETMS		

Table 9. Economic Analysis of Four Aircraft on Respective Popular Routes

Money Saved Per Flight on Most Popular Routes		
Airframe	***Case***	
	Low	
	70% SWNT Scenario 1	***70% SWNT Scenario 2***
747-400	$1,460.56	$4,035.03
757-200	$333.25	$720.70
A320	$130.92	$164.14
E145	$6.68	$37.41
	Nom	
	70% SWNT Scenario 1	***70% SWNT Scenario 2***
747-400	$391.44	$9,535.57
757-200	$236.71	$616.37
A320	$122.55	$150.44
E145	$6.79	$32.32
	Hi	
	70% SWNT Scenario 1	***70% SWNT Scenario 2***
747-400	$159.98	x
757-200	$220.93	x
A320	$132.06	$149.56
E145	$4.36	$20.71
Sources:	***Fuel Cost*** : 2003 Bureau of	
	Transportation Statistics	
	Route Length : ETMS	

III. Conclusion

The analysis presented considered notional Boeing 747-400 and 757-200, Airbus A320, and Embraer E145 with carbon nanotube reinforced polymer (CNRP) as the primary structural material, replacing the entire volume of structural aluminum with CNRP, without including any modifications to the geometry or design of the airframe.

Those benefits include a notable reduction in mass at takeoff, M_{AT}, for each airframe in each weight classification. Each airframe modeled saw an average 17.32% weight reduction in the low initial takeoff mass category, with a minimum mass reduction in the high initial takeoff mass category of over 10%.

Consequential benefits exist due to the mass reduction found in the notional CNRP-structured airframe analysis, including increases in aircraft flight range and cruise altitude, and a decrease in fuel consumption, which directly correlate to more economical flights. The most significant increase in flight range observed by the notional CNRP-structured Embraer 145, cruising at a higher altitude, traverses 36% farther than its contemporary counterpart. The average fuel savings for all CNRP-structured airframes is 9.8%, with the maximum fuel savings of the group found with the low initial takeoff mass CNRP-structured Embraer 145, saving 32.9% more fuel than its contemporary counterpart and cruising at a higher altitude. These benefits translate to savings for the air carrier maintaining fleets of these aircraft, especially for fuel expenditures. The CNRP-structured 747-400, for example, saves an estimated $10k per flight on the 5,676 nautical mile route from Los Angeles (LAX) to Seoul, Korea (ICN) due to the decrease in fuel consumption in the flight modeled.

Though the probability of CNRP-structured contemporary airframes is unlikely, this type of analysis provides insight into a small group of benefits seen by a nano-structured material applied on the macro scale.

Acknowledgments

The authors wish to extend thanks to Alison Reynolds, Brian Noguchi, Agnieszka Koscielniak, David Smith and Jason Giovannelli for their contributions to the project. Thanks to technical advisors Dr. James Ellenbogen, Brigitte Rolfe, David Maroney and Doyle Peed. And special thanks to MITRE CAASDs Chief Engineer Dr. Glenn Roberts for initiating the project with Dr. James Ellenbogen and to Charlotte Laqui for her mentorship.

References

[1]Shackelford, J.F, *Introduction to Materials Science for Engineers*, 5 ed. Prentice Hall, Upper Saddle River, 2000.

[2]"747-400 Fun Facts", Boeing Commercial Airplanes Online Technical Specifications, Parts, URL: http://www.boeing.com/commercial/747family/pf/pf_facts.html [cited March 2002].

[3]Sweetman, B. "Boeing 7E7 Composites," Paris Air Show 2003, AviationNow Show News Online, *Aviation Week*, URL: www.aviationweek.com/shownews/03paris/topstor08.htm [cited November 2003].

[4]"Boeing's New 7E7 to be 50% Composite," Netcomposites Newsroom, URL: www.netcomposites.com/news.asp?1867 [cited November 2003].

[5]Ijima, S. "Helical Microtubules of Graphitic Carbon." *Nature*, vol. 354, 1991, pp. 56-58.

[6]Chang, K."It Slices! It Dices! Nanotube Struts Its Stuff," *New York Times*. New York, July 16 2002.

[7]Krishnan, A., Dujardin, E., Ebbesen, T. W., Yianilos, P. N., and M. M. J. Treacy, "Young's Modulus of Single-Walled Nanotubes," *Physical Review B*, vol. 58, 1998, pp. 14013-14019.

[8]Pipes, R. B., S. J. V. Frankland, P. Hubert, and E. Saether, "Self-consistent Physical Properties of Carbon Nanotubes in Composite Materials," NASA/CR-2002-212134, 2002.

[9]Qian, D., G. J. Wagner, W. K. Liu, M. F. Yu, and R. S. Ruoff, "Mechanics of Carbon Nanotubes," *Applied Mechanics Review*, vol. 55, 2002, pp. 495-533.

[10]Köhler, T., and F. Vollrath, "Thread biomechanics in the two orb-weaving spiders Araneus diadematus (Araneae, Araneidae) and Uloboris walckenaerius (Araneae, Uloboridae)." *Journal of Experimental Zoology*, vol. 271, 1995, pp. 1-17.

[11]Penumadu, D., A. Dutta, G. M. Pharr, and B. Files, "Mechanical Properties of Blended Single Wall Carbon Nanotube Composites," *Journal of Materials Research*, vol 18, no 8, 2003, pp 1849-1853.

[12]Hadjiev, V. G., M. N. Iliev, S. Arepalli, P. Nikolaev, and B. S. Files, "Raman Scattering Test of Single-Wall Carbon Nanotube Composites," *Applied Physics Letters*, vol 78, no 21, 2001, pp 1-3.

[13]Kumar, S., T. D. Dang, F. E. Arnold, A. R. Bhattacharyya, B. G. Min,X. Zhang, R. A. Vaia, C. Park, W. W. Adams, R. H. Hauge, R. E. Smalley, S. Ramesh, and P. A. Willis, "Synthesis, Structure, and Properties of PBO/SWNT Composites," *Macromolecules*, vol 35, 2002, pp 9039-9043.

[14]Saito, R., M. Fujita, G. Dresselhaus, M.S. Dresselhaus, "Electronic-Structure of Chiral Graphene Tubules based on C_{60}," *Physical Review B*, vol. 46, no. 3, 1992, pp 1804-1811.

[15]Gao, G., T. Çagin, and W. A. Goddard, "Energetics, structure, mechanical and vibrational properties of single-walled carbon nanotubes," *Nanotechnology*, vol. 9, 1998, pp. 184-191.

[16]Yu, M.F. B. S. Files, S Arepalli, and R. S. Ruoff, "Tensile Loading of Ropes of Single Wall Carbon Nanotubes and Their Mechanical Properties," *Physical Review Letters*, vol. 84, 2000, pp. 5552-5555.

[17]Louie, S. G.,"Electronic properties, junctions, and defects of carbon nanotubes," *Carbon Nanotubes, Topics in Applied Physics* vol. 80, edited by M. S. Dresselhaus, G. Dresselhaus, and P. Avouris, Springer-Verlag, Heidelberg, 2001, pp. 113.

[18]White, C. T., and T. N. Todorov, "Carbon Nanotubes as Long Ballistic Conductors," *Nature*, vol 393, pp 240-242, 1998.

[19]Frank, S. P., P. Poncharal, Z. L. Wang, W. A. de Heer, "Carbon Nanotube Quantum Resistors", *Science*, vol 280, 1998, pp. 1744-1746.

[20]Frankland, S. J. V., T. Bandorawalla, and T. S. Gates, "Calculation of Non-Bonded Forces Due to Sliding of Bundled Carbon Nanotubes," *Proceedings of 44th AIAA/ASME/AHS Structures, Structural Dynamics, and Materials Conference*, AIAA 2003-1536, American Institute for Aeronautics and Astronautics, Norfolk, VA, 2003.

[21]Yu, M. F., O. Lourie, M. J. Dyer, K. Moloni, T. F. Kelly, and R. S. Ruoff, "Strength and Breaking Mechanism of Multiwalled Carbon Nanotubes Under Tensile Load," *Science*, vol. 287, 2000, pp. 637-640.

[22]Yu, M. F., B. I. Yakobson, and R. S. Ruoff, "Controlled Sliding and Pullout of Nested Shells in Individual Multiwalled Carbon Nanotubes," *Journal of Physical Chemistry B*, vol. 104, 2000, pp. 8764-8767.

[23]Dow Chemical Company, "Dow HDPE 65053N High Density Polyethylene," *MatWeb Material Property Data*, 2003, URL: http://www.matweb.com/search/SpecificMaterial.asp?bassnum=PDW483 [cited August 2003]

[24]Agarwal, B. D., and L. J. Broutman, *Analysis and Performance of Fiber Composites*, 2nd ed: John Wiley & Sons, Inc., 1990.

[25]Reynolds, A., Final Briefing of MITRE NanoSystems Group, August 2001.

[26]Kollár, L. P., and G. S. Springer, *Mechanics of Composite Structures*, Cambridge: Cambridge University Press, 2003.

[27]*Metals Handbook, Properties and Selection: Irons, Steels, and High Performance Alloys*, Vol. 1. ASM International, 10th Ed., 1990.

[28]*Materials Properties Handbook: Titanium Alloys*, edited by R. Boyer, G. Welsch, and E. W. Collings, ASM International, Materials Park, 0H, 1994.

[29]Raymer, D. P., *Aircraft Design: A Conceptual Approach*, 3rd ed. Reston: American Institute of Aeronautics and Astronautics, 1999.

[30]*Metals Handbook, Properties and Selections: Nonferrous Alloys and Special-Purpose Materials*, Vol. 2., ASM International 10th Ed., 1990.

[31]Ajayan, P. M., L. S. Schandler, C. Giannaris, and A. Rubio, "Single-Walled Carbon Nanotube Composites: Strength and Weakness," *Advanced Materials*, vol. 12, 2000, pp. 750-753.

[32]Sandler, J., M. S. P. Shaffer, T. Prasse, W. Bauhofer, K. Schulte, and Windle, A. H.,"Development of a Dispersion Process for Carbon Nanotubes in an Epoxy Matrix and the Resulting Electrical Properties," *Polymers*, vol. 40, 1999, pp. 5967-5971.

[33]Schandler, L. S., S. C. Giannaris, and P. M. Ajayan, "Load Transfer in Carbon Nanotube Epoxy Composites," *Applied Physics Letters*, vol. 73, 1998, pp. 3842-3844.
[34]Qian, D., E. C. Dickey, R. Andrews, and T. Rantell, "Load Transfer and Deformation Mechanisms in Carbon Nanotube-Polystyrene Composites," *Applied Physics Letters*, vol. 76, 2000, pp. 2868-2870.
[35]Vergano, D., "Researchers Spin Super-Powerful Fiber," *USA Today*, June 11, 2003
[36]Yoon, C. K., "Those Intriguing Nanotubes Create the Toughest Fibers Known," *The New York Times*. New York, 2003, pp. D3.
[37]Dalton, A. B., S. Collins, E. Munoz, J. M. Razal, V. H. Ebron, J. P. Ferraris, J. N. Coleman, B. G. Kim, and R. H. Baughman, "Super-tough carbon-nanotube fibres," *Nature*, vol. 423, 2003, pp. 703.
[38]Gates, T. S., and J. A. Hinkley, "Computational Materials: Modeling and Simulation of Nanostructured Materials and Systems," NASA/TM-2003-212163, 2003.
[39]EUROCONTROL Experimental Centre, "User Manual for the Base of Aircraft Data (BADA) – Revision 3.4," European Organization for the Safety of Air Navigation, June 2002.
[40]The Boeing Company. Airport Manual for 747-400. D6-58326-1.
[41]Asselin, M., *An Introduction to Aircraft Performance*, Reston: AIAA, 1997.
[42]Enhanced Traffic Management System (ETMS), The Volpe National Transportation Systems Center, Department of Transportation.
[43]2003 Bureau of Transportation Statistics, URL: http://www.bts.gov/oai/fuel/fuelyearly.html. [cited June 2004]